

Support Information

Heterogeneous Photocatalyzed Acceptorless Dehydrogenation of 5-Hydroxymethylfurfural upon Visible-Light Illumination

Wanying Liang ‡, Rui Zhu ‡, Xinglong Li, Jin Deng*, Yao Fu*

Hefei National Laboratory for Physical Sciences at the Microscale, CAS Key Laboratory of Urban Pollutant
Conversion, Anhui Province Key Laboratory of Biomass Clean Energy, Center for Excellence in Molecular
Synthesis of CAS, University of Science and Technology of China, Hefei 230026.

Institute of Energy, Hefei Comprehensive National Science Center, Hefei 230031

I . General

1. Materials

All the chemicals were commercially available and used without further purification. The reagents needed for the experiment were: urea, melamine, tetraethyl orthosilicate, hydrochloric acid (HCl), hydrofluoric acid (HF), nickel chloride hexahydrate ($\text{NiCl}_2 \cdot 6\text{H}_2\text{O}$), iron chloride hexahydrate ($\text{FeCl}_3 \cdot 6\text{H}_2\text{O}$), cobalt chloride hexahydrate ($\text{CoCl}_2 \cdot 6\text{H}_2\text{O}$), dichloroethane, methanol (MeOH), ethanol (EtOH), and acetonitrile (MeCN). Among them, 5-hydroxymethylfurfural (HMF) was synthesized by Hefei Leaf Biotech Co., Ltd.

2. Characterization

The BET specific surface area and N_2 adsorption-desorption isotherms of samples were measured at 77 K (Tristar II 3020M, Micromeritics, America). Sample pre-activation procedure: degas at 120°C for 2 h and then activate at 300°C for 2 h. The sample weight after activation was 0.1g. According to the N_2 adsorption/desorption isotherm, the specific surface area and pore size distribution of the catalyst were calculated by BET and BJH methods, respectively.

An inductively coupled plasma optical emission spectrometer (ICP-OES, Optima 7300 DV, PerkinElmer, America) was used to analyze the actual loading amount of metal Ni in the sample. The characteristic wavelength of Ni was 221.647 nm, and the Ni concentration in the sample was calculated by using the characteristic peak. The solid sample preparation: 50mg of the catalyst dissolved in aqua regia, heated it close to 500°C , distilled water was added continuously to the digester all solids dissolved to prepare a homogeneous solution of 100mL. Measured Ni concentration in the solution was calculated to give the supported Ni catalyst mass fraction. Liquid sample preparation method: Take 1mL of reaction solution and filter, heated nearly 500°C , and continuously add distilled water to cook to prepare 100mL homogeneous solution. Measured Ni concentration in the solution was calculated to obtain a reaction filtrate loss Ni content.

The X-ray diffraction patterns (XRD) of the powder samples were detected by the multi-function rotating target X-ray diffractometer (SmartLab), using $\text{Cu K}\alpha$ radiation at 40 kV and 150 mA. The 2θ range was 5° to 80° , and the step length was 0.02° .

SEM was mainly used to observe the microscopic appearance and size of the sample (GeminiSEM 500, Carl Zeiss AG, Germany). The accelerating voltage was 0.02-30 kV, resolution(Mn Ka) was 127 eV, equipped with an EDX spectrometer. The specific test process was as follows: Dip a small amount of sample with a cotton swab, smeared

it on the black conductive adhesive, and sprayed gold before testing.

TEM and EDS mapping were mainly used to observe the microscopic appearance and element distribution of samples (JEM-2100 Plus, HT7700 Exalens, JEOL Ltd., Japan). Point resolution: 0.23 nm; fringe resolution: 0.14 nm; acceleration voltage: 200 kV; magnification: $30\sim 1.5\times 10^6$; tilt angle: $\pm 30^\circ$; element analysis range: 5B ~ 92U; camera: SIS QUEMESA 11 million pixels Bottom inserted CCD. Sample preparation process: a small amount of catalyst was dispersed in ethanol and spot coated on qualitative filter paper.

X-ray photoelectron spectroscopy experiments were performed on ESCALAB 250Xi (Thermo Scientific, England) spectrometer. Test conditions: ultimate vacuum of analysis chamber: 5×10^{-10} mbar; monochromatic X-ray source: Al $K\alpha$ 150 W, beam spot 500 μm ; Energy resolution and sensitivity: when the FWHM of $\text{Ag}3d_{5/2}$ is 0.6 eV, the intensity is greater than 1,600,000 cps. The C1s photoelectron peak with binding energy of 284.8 was used as a reference to correct the spectrum.

II . Experimental

1. Preparation of graphitic carbon nitride

The mesoporous graphitic carbon nitride was synthesized according to a previous work. Briefly, about 10 g urea were dissolved in a solution of 0.2 M HCl solution (15 mL) and ethanol (13 mL) under vigorous stirring, and tetraethyl orthosilicate (8 mL) was then slowly added to the above solution drop by drop. After stirring vigorously at room temperature for 3 h, the mixture was heated under vacuum for the solvent evaporation and then dried at 100 °C for about 12 h. The obtained white solid was heated at 550 °C for 4 h (heating rate: 2.5 °C/min) under nitrogen atmosphere. Subsequently, hydrofluoric acid was used to remove SiO_2 . Then, the obtained pale-yellow solid was washed with water and ethanol for several times and dried at 80 °C for about 12h. The pale-yellow solid (about 4 g) was finally obtained and denoted as ACN.

The graphitic carbon nitride was synthesized according to a previous work. About 10 g urea or melamine was directly heated at 550 °C for 4 h (heating rate: 2.5 °C/min) under nitrogen atmosphere, giving a pale-yellow solid. Among them, the support prepared from urea was named BCN, and the support prepared from melamine was named CCN.

2. Preparation of Ni/ACN, Ni/BCN, Ni/CCN, Fe/ACN, Co/ACN

The Ni/ACN photocatalysts was synthesized by photodeposition method. In detail,

the photodeposition step was performed in the 200mL glass flask. The prepared ACN sample (150 mg) was dispersed in 50 mL dichloroethane solution, containing 18mg nickel chloride hexahydrate ($\text{NiCl}_2 \cdot 6\text{H}_2\text{O}$) and 3.2 mL methanol. Then, the system was evacuated and flushed with nitrogen to replace the residual air. This suspension was stirred and irradiated for 12 h under 390nm light. After that, the product was filtered and washed with distilled water, and finally dried in a vacuum at 60 °C overnight. Series of catalysts could be synthesized by changing the types of metal precursors and supports, which was denoted as Ni/ACN, Ni/BCN, Ni/CCN, Fe/ACN, Co/ACN, respectively. Regarding the dosage of $\text{NiCl}_2 \cdot 6\text{H}_2\text{O}$, $\text{CoCl}_2 \cdot 6\text{H}_2\text{O}$ and $\text{FeCl}_3 \cdot 6\text{H}_2\text{O}$: 150mg support corresponding to 18mg $\text{NiCl}_2 \cdot 6\text{H}_2\text{O}$, 18mg $\text{CoCl}_2 \cdot 6\text{H}_2\text{O}$ and 22mg $\text{FeCl}_3 \cdot 6\text{H}_2\text{O}$.

Photodeposition step was performed in the 200mL glass flask, as the Fig.S1 showed. The glass flask was purchased from Beijing synthware Glass Co., Ltd (www.xinweier.com). The glass material is Pyrex glass, which is a borosilicate glass with an expansion coefficient of $(3.3 \pm 0.1) \times 10^{-6} / \text{K}^{-1}$.



Fig.S1. The photo of the glass flask.

The Photo Reaction Setup (SCI-PCRS-3-455) was purchased from Anhui Kemi machinery technology Co., Ltd. (www.kemiyiqi.com). The inside of the light reaction device is covered with mirrors (Fig.S2A). The distance from the edge of the light source to the edge of the reaction tube is 10 cm (Fig.S2B). The photoreaction device we purchased was equipped with a refrigeration device, which could precisely control the reaction temperature at 26 °C during the reaction process.

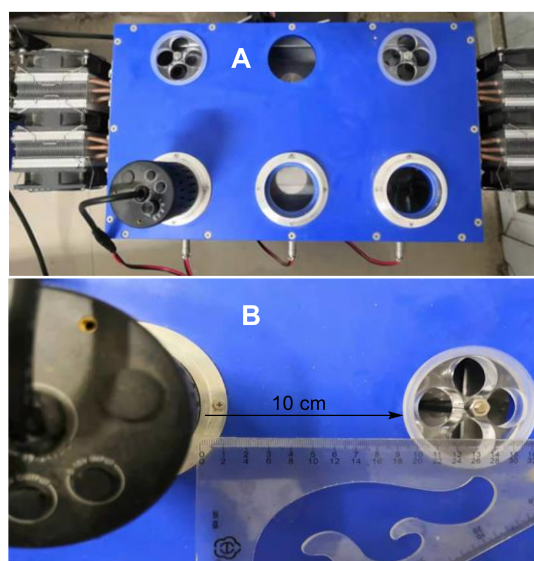


Fig.S2. (A) Top view of photoreaction device with refrigeration device. (B) The distance from the edge of the light source to the edge of the reaction tube.

We used Kessil PR160L LED PhotoReaction Lighting (www.kessil.com). Kessil LED lamp had high output, precise wavelength and strong penetrating power. It could precisely control the wavelength of the light source within the required wavelength $\pm 5\text{nm}$ range. Technical Specifications of the Kessil LED lamp are listed in the table below. The lamp emission spectrum is shown in the Fig.S3B.

Table.S1. Technical Specifications of the Kessil LED lamp.

Specifications	
Power Consumption	370nm (max 43W), 390nm (max 52W), 427nm & 440nm (max 45W), 456nm (max 50W), 467nm (max 44W), 525nm (max 44W)
Input Voltage	100-240 VAC
Operating Temperature	0 - 40°C / 32 - 104°F
Beam Angle	56°
Wavelength Options	370nm, 390nm, 427nm, 440nm, 456nm, 467nm, 525nm
Average Intensity of PR160 series	352mW/cm ² (measured from 1 cm distance)
Dimensions	4.49" x 2.48" / 11.4cm x 6.3cm (H x D)

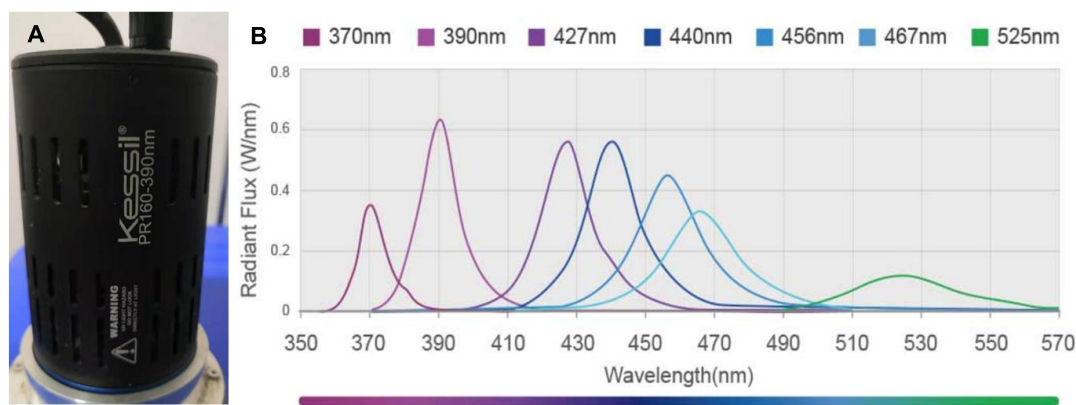


Fig.S3. (A) Kessil PR160L LED PhotoReaction Lighting. (B) The lamp emission spectrum

3. Photocatalytic reaction

The Photo Reaction Setup (SCI-PCRS-3-455) was purchased from Anhui Kemi machinery technology Co., Ltd. The photocatalytic hydrogen production system was performed in a 10 mL glass flask. Specific steps: 0.05 mmol HMF and 10 mg Ni/ACN were dispersed in acetonitrile (MeCN) solution (1 mL). This system was evacuated and flushed with nitrogen to replace the residual air. Then, the photocatalytic system was irradiated under 390nm light and magnetic stirring.

Recycling experiment of Ni/ACN photocatalyst was also tested, maintaining the same reaction conditions as those described above, except using the recovered catalyst. For each time, the used catalyst was separated from the reaction system by centrifugation. The obtained catalyst was then washed with methanol for a few times and dried at 60 °C overnight, prior to its reuse in another run.

Photocatalytic reaction was performed in the 10mL glass flask, as the Fig.S4A showed. The glass flask was purchased from Beijing synthware Glass Co., Ltd (www.xinweier.com). The glass material is Pyrex glass, which is a borosilicate glass with an expansion coefficient of $(3.3 \pm 0.1) \times 10^{-6} / \text{K}^{-1}$.

The Photo Reaction Setup (SCI-PCRS-3-455) was purchased from Anhui Kemi machinery technology Co., Ltd. (www.kemiyiqi.com). The photoreaction device we purchased was equipped with a refrigeration device, which could precisely control the reaction temperature at 26 °C during the reaction process. We used Kessil PR160L LED PhotoReaction Lighting (www.kessil.com) during the photocatalytic reaction. Technical Specifications of the Kessil LED lamp are listed in the Table.S1. The lamp emission spectrum is shown in the Fig.S3B.

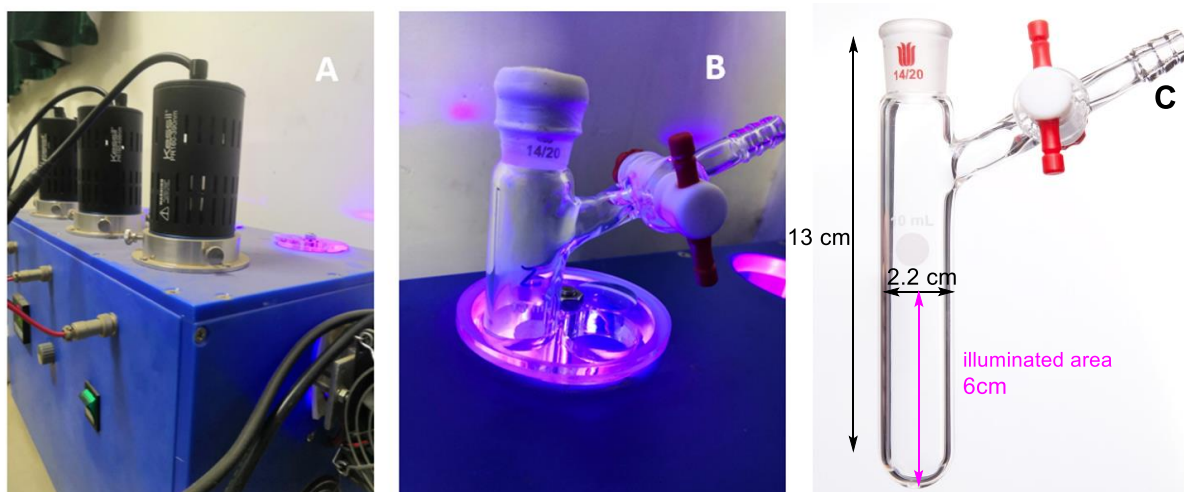
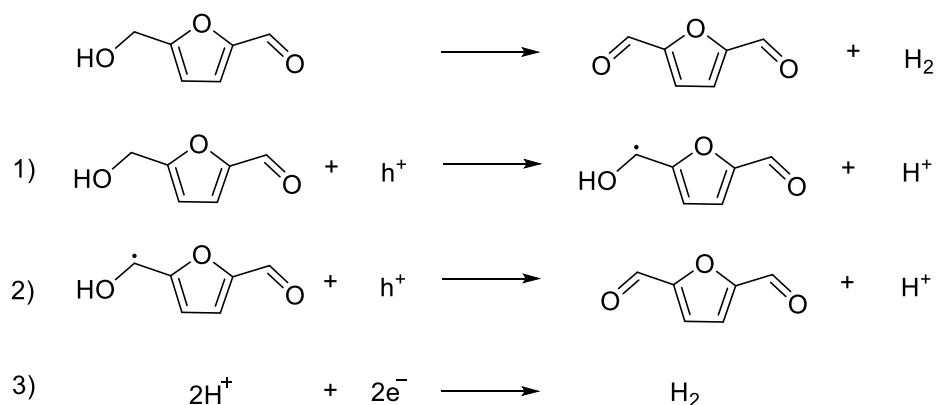


Fig.S4. The photocatalytic reaction Setup. (A) photo of the photoreaction device, (B) photo of the glass schlenk flask under UV-LED, (C) photo of the glass schlenk flask.

4. Determination of conversion and yield

The reaction equation and semi-reaction equation of HMF dehydrogenation are shown in Scheme S1. In this reaction system, whenever a molecule of HMF undergo a dehydrogenation reaction to generate a molecule of DFF and hydrogen, there would be two electrons involved in the reaction.



Scheme.S1. The reaction equation and semi-reaction equation of HMF dehydrogenation

The conversion and yield of target product were analyzed by High Performance Liquid Chromatography (HPLC) analysis. High Performance Liquid Chromatography (HPLC): Waters e2695 HPLC; column: Waters C18(5 μm 250 mm 4.6 mm); mobile phase: acetonitrile: 0.5 wt.% trifluoroacetic acid aqueous (30:70, v/v); flow rate: 1 mL/min; column temperature: 30 $^\circ\text{C}$; detector: Waters 2489UV/Vis Detector; detection wavelength: 264 nm.

HPLC sample preparation process: Dilute 1mL reaction solution to 100mL, filter and

retain the filtrate. Taking into account that the peak area of HPLC was directly proportional to the concentration of the substance, the standard curve method was used to determine the concentration of substrate and product in the reaction solution (external standard method). The standard curve was calculated by measuring a series of standard sample solutions with decreasing concentration gradient., as shown in Fig.S5A. The retention time of 5-hydroxymethyl furfural was 2.688, and the retention time of 2,5-furandiformaldehyde was 3.471, as shown in Fig.S5B.

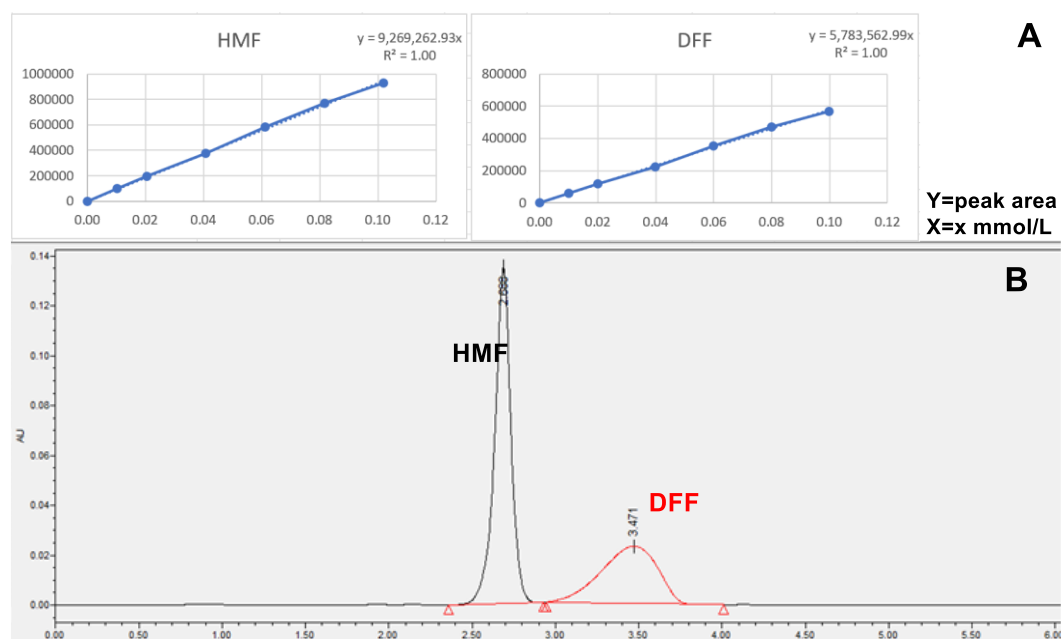


Fig.S5. (A) standard curve line of HMF and DFF, (B) HPLC of HMF and DFF.

The HMF conversion and DFF yield were calculated as follows:

$$\text{Conversion (\%)} = \frac{\text{Moles of feedstock consumed}}{\text{Moles of feedstock input}} \times 100\%$$

$$\text{Product yield (\%)} = \frac{\text{Moles of product}}{\text{Moles of feedstock input}} \times 100\%$$

5. Determination of the apparent quantum yield

The apparent quantum efficiency (AQE) was measured under the same photocatalytic reaction condition. The number of incident photons was measured by Iron(III) potassium oxalate trihydrate [potassium tris(oxalato)ferrate(III) trihydrate] $K_3[Fe(C_2O_4)_3] \cdot 3H_2O$, photoreduction (Hatchard–Parker actinometer, commonly called ferrioxalate actinometer).

Following a similar procedure reported by references ^[1], an aqueous solution of potassium ferrioxalate was prepared and stored in the dark. All procedures should be

done under red safe-light. Green crystals of $K_3[Fe(C_2O_4)_3] \cdot 3H_2O$ were prepared by mixing 3 vol 1.5 M $K_2C_2O_4$ with 1 vol 1 M $FeCl_3$ solution, recrystallized three times from warm water, dried at 45 °C and kept in the dark. 0.006 and 0.01M solutions were used for actinometry.

A 0.006 M solution was prepared by dissolving 2.947 g of the crystals in 100 mL H_2SO_4 (0.5 M) and dilution with distilled water to 1 L. An absorption spectrum of the solution was taken. Total absorption at the desired irradiation λ and optical pathlength was recommended. For example, 2 mL (V_1) of the solution were irradiated under efficient stirring. 1 mL (V_2) of the irradiated solution was given into a 10 mL (V_3) volumetric flask containing a mixture of 4 mL 0.1 % 1.10-phenanthroline solution (store in the dark) and 0.5 mL buffer (stock solution: 82 g $NaC_2H_5CO_2$, 10 mL conc. H_2SO_4 , diluted to 1 L with distilled water) which was then diluted to the mark with distilled water. It was essential that the irradiation time measurement (electronic shutter) as well as the pipetting was done very precisely. A reference was prepared in the same way except that it had not been irradiated. Both solutions were kept in the dark (about an hour) until full color development was achieved, and the absorbance difference between the two samples was measured at 510 nm [optical pathlength $l = 1$ cm, $\epsilon(510 \text{ nm}) = 11\ 100 \text{ dm}^3 \text{ mol}^{-1} \text{ cm}^{-1}$]. A 0.01 M solution was prepared as above. The 0.006M photometer was used to measure the number of incident photons from 370/390/427/440nm light sources, and the 0.01M photometer was used to measure the number of incident photons from 456/467nm light sources. The photon flux, amount basis, $q_{n,p}/\text{einstein s}^{-1}$, entering the sample cell was given by (in coherent SI units):

$$q_{n,p} = \frac{\Delta A V_1 V_3}{\Phi(\lambda) \epsilon(510 \text{ nm}) V_2 l t}$$

with $t =$ irradiation time. At room temperature, $\Phi(\lambda) = 1.14$ (0.006 M) at 405 nm, 1.11 (0.006 M) at 436 nm, 1.12 (0.01 M) at 458 nm. The Incident electrons numbers of 370/390nm take the $\Phi(405 \text{ nm}) = 1.14$ (0.006 M) as a reference, 427/440nm take the $\Phi(436 \text{ nm}) = 1.11$ (0.006 M) as a reference, and 456/467nm take the $\Phi(458 \text{ nm}) = 1.12$ (0.01 M) as a reference. There was no total absorption above 450 nm even in 0.15 M solution. In this case, the value of the photon flux must be divided by the fraction of absorbed light at the irradiation wavelength ($1-10^{-A}$).

The following table lists the number of incident photons of the measured light source with different wavelengths as a reference.

Table.S1. Incident electrons numbers of the measured light sources with different wavelengths.

Wavelength (nm)	Incident electrons numbers (*10 ²⁰ 12h)
370	2.11
390	3.80
427	7.26
440	12.21
456	13.52
467	7.43

The AQE was calculated according to the following formula.

$$\text{AQE (\%)} = \frac{\text{number of reacted electrons}}{\text{number of incident electrons}} \times 100\%$$

[1] H. J. KUHN, S. E. BRASLAVSK and R. SCHMIDT, *Pure Appl. Chem.*, 2004, **76**, 2105–2146.

6. Deconvolution processing of Ni XPS

According to the rules in < Handbook of X-ray Photoelectron Spectroscopy > [2], the Ni XPS peaks were deconvoluted in order to determine the amount of Ni²⁺ and Ni⁰:

Table.S2. The amount of Ni²⁺ and Ni⁰ on sample surface determined by XPS.

Catalyst	Ni species	Binding energy (eV)	Content (%)
Ni/ACN fresh	Ni ⁰ 2p _{3/2}	853.5	8.37
	Ni ²⁺ 2p _{3/2}	856.3	10.91
Ni/ACN recycled	Ni ⁰ 2p _{3/2}	853.3	7.88
	Ni ²⁺ 2p _{3/2}	856.4	9.58
Ni/ACN in suit	Ni ⁰ 2p _{3/2}	853.6	6.63
	Ni ²⁺ 2p _{3/2}	856.2	11.21

[2] J.F. Moulder, W. F. Stickle, P. E. Sobol, K. D. Bomben, *Handbook of X-ray Photoelectron Spectroscopy*, USA, 1992.

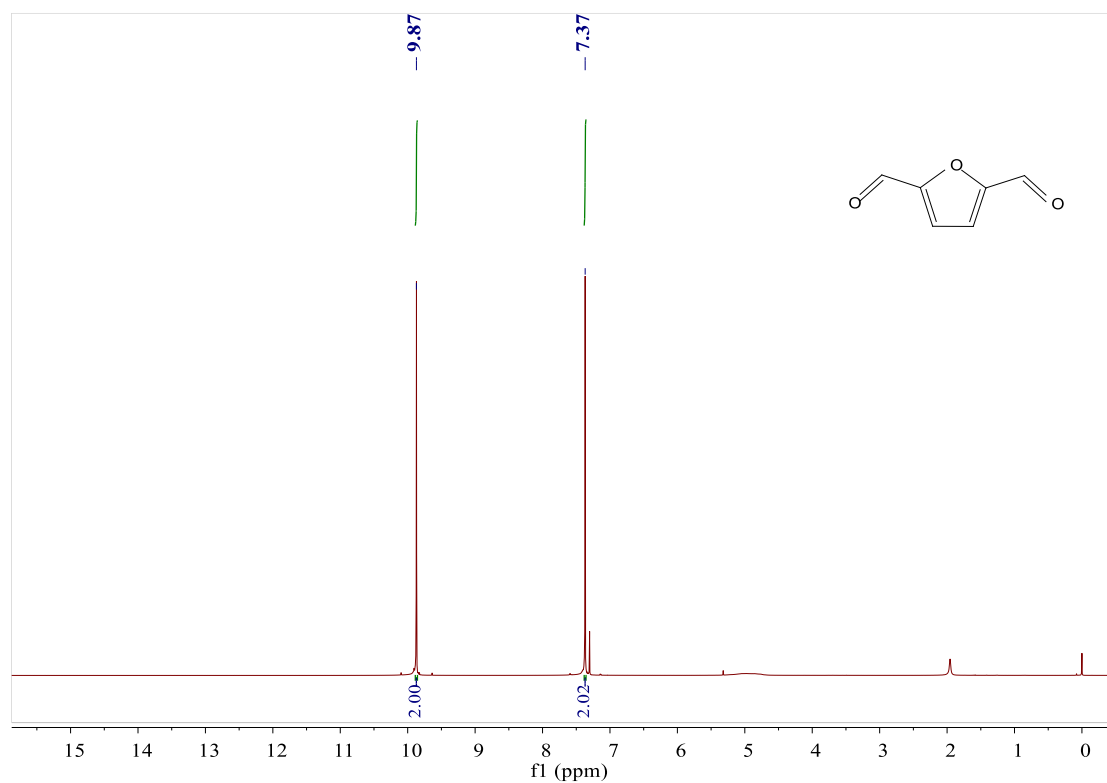
7. NMR spectrum data

¹H-NMR and ¹³C-NMR spectra were recorded on a Bruker Avance 400 spectrometer at ambient temperature. Multiplicities are described using the following

abbreviations: chemical shift (ppm, scale), multiplicity (s = singlet, d =doublet, t = triplet, q = quartet, m = multiplet and/or multiplet resonances, br = broad), coupling constant (Hz), and integration. Carbon chemical shifts are reported in ppm (δ) relative to TMS with the solvent resonance as the internal standard (CDCl_3 , δ 77.16 ppm). NMR data were collected at 25 °C. NMR spectra were processed using MestReNova.

^1H NMR (400 MHz, Chloroform-*d*) δ 7.37(s, 2H), 9.87(s, 2H).

^{13}C NMR (101 MHz, Chloroform-*d*) δ 119.38, 154.19, 179.25.



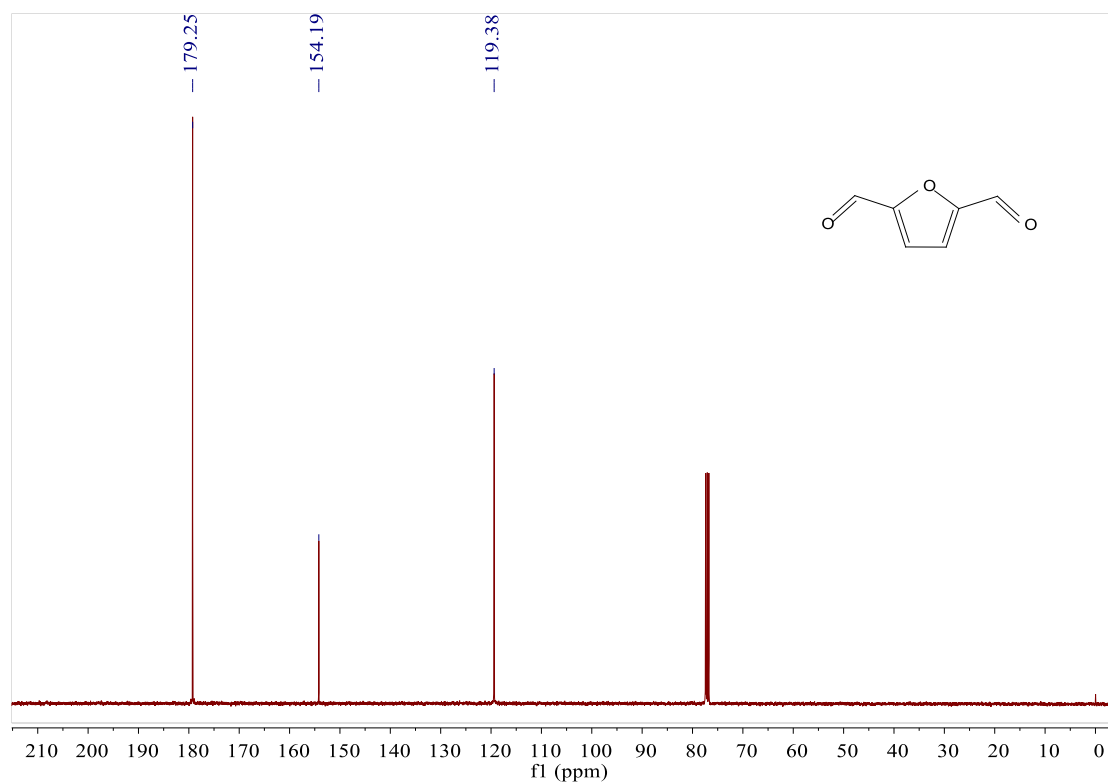


Fig.S6. NMR spectrum data of DFF.

8. The effect of the solvent on the reaction

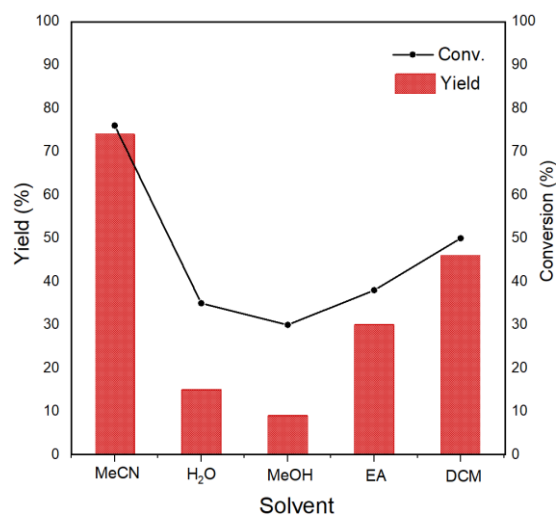


Fig.S7. Variation of solvent. Reaction conditions: HMF 0.05mmol/mL; temperature = 25°C; light wavelength = 390 nm; N₂ and reaction time = 12 h.

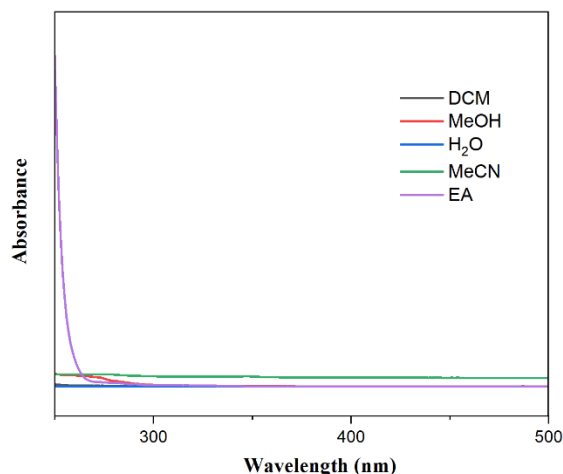


Fig.S8. UV-vis DRS of solvent.

A series of solvents were adopted to investigate the solvent effect on the photocatalytic dehydrogenation of HMF. As shown in Fig.S7, MeCN (acetonitrile) was the optimal solvent obtaining 76% conversion of HMF and 74% yield of DFF. When using other solvents, the yield of the product was low. Explore the reasons for the difference in reactivity in different solvents: when using water as a solvent, water was used as an electron acceptor, and HMF was used as a sacrificial agent; its primary oxidation products, DFF, could be further oxidized to carboxylic acid because of the presence of water. Therefore, the selectivity was poor in the aqueous system. When methanol was used as a solvent, the competitive reaction between methanol and HMF made the conversion of HMF very poor. Methanol would generate formaldehyde under photocatalysis, and even further coupling to generate acetal. Not only that, methanol could also act as a hole scavenger to inhibit the progress of the reaction. In addition, we found that when the solvent contained O, such as water (H₂O), methanol (MeOH) and ethyl acetate (EA) as the solvent, the reaction conversion was poor, which may be related to the electronegativity of the solvent. When using dichloromethane (DCM) as the reaction solvent, we obtained experimental result second only to MeCN solvent.

Moreover, we detected the UV-Vis absorption patterns of solvents used in Fig.S7. As can be seen from Fig.S8, in this manuscript, the various solvents used in Fig.S7 have little absorption under a light source with a wavelength of 350-500 nm. Therefore, the influence of the UV-Vis absorption patterns of the solvent on the reaction can be excluded.

9. Experiment to verify H₂ generation

In the supplementary verification reaction, we also measured the production of hydrogen. The photocatalytic hydrogen production system was performed in a 10 mL glass flask. Specific steps: 0.05 mmol HMF and 10 mg Ni/ACN were dispersed in acetonitrile (MeCN) solution (1 mL). This system was evacuated and flushed with nitrogen to replace the residual air. Then, the photocatalytic system was irradiated under 390nm light and magnetic stirring. The sampling test method refers to the process in the previous work.^[3]

A TCD (thermal conductivity detector) for analysis of H₂ on TDX-01 column. Gas chromatographic (GC): Panna A91 Plus GC; column: TDX-01; column temperature: 60 °C.

A possible quantification of hydrogen was revealed a best qualitative guess of 80% of DFF's yield. This may be caused by systematic errors, manual sampling errors and calculation errors.

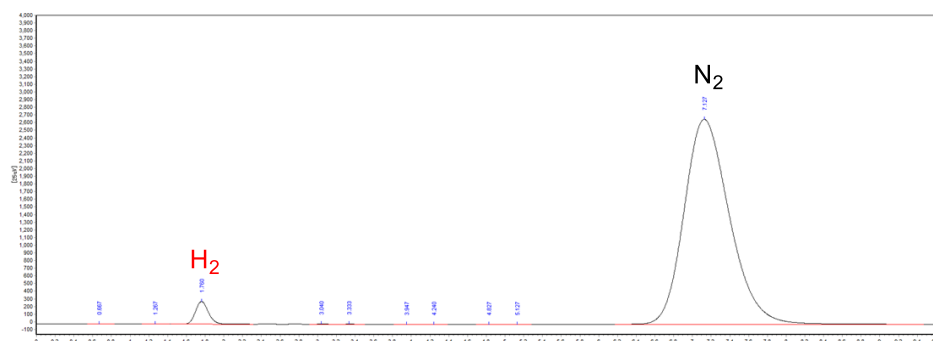


Fig.S9. GC of H₂.

[3] K. Khan, X. Tao, Y. Zhao, B. Zeng, M. Shi, N. Ta, J. Li, X. Jin, R. Li and C. Li, *J. Mater. Chem. A*, 2019,**7**, 15607-15614.

10. Scavenger study

A series of scavengers have been studied. Two scavengers were selected to quench holes (KI, Potassium Iodide) and electrons (C₆H₅NO₂, Nitrobenzene).

Experiment procedure: The Photo Reaction Setup (SCI-PCRS-3-455) was purchased from Anhui Kemi machinery technology Co., Ltd. The photocatalytic hydrogen production system was performed in a 10 mL reaction tube. Specific steps: 0.05 mmol HMF and 10 mg Ni/ACN were dispersed in acetonitrile (MeCN) solution (1 mL). Added 2 mmol/mL of KI, C₆H₅NO₂ respectively. This system was evacuated and flushed with nitrogen to replace the residual air. Then, the photocatalytic system was irradiated under UV-vis light and magnetic stirring. The results are shown in the figure below.

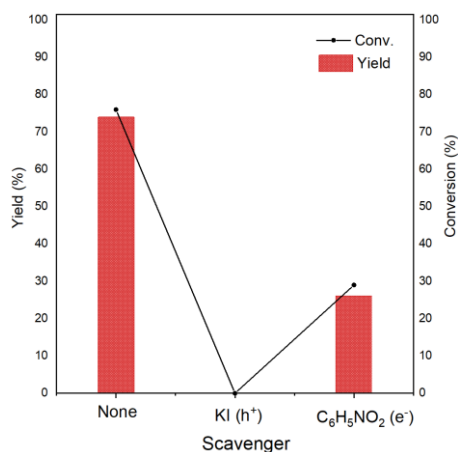


Fig.S10. Scavenger study. Reaction conditions: HMF 0.05mmol/mL; scavenger 2mmol/mL; temperature = 25°C; light wavelength = 390 nm; solvent = MeCN; N₂ and reaction time = 12 h.

The above results showed that after KI was added, the holes were quenched and HMF was no longer transformed, indicating that the photogenerated holes played a leading role in the reaction. In the solvent screening reaction, the same result occurred when methanol was used as the solvent. This is because methanol not only formed a competitive reaction with HMF, but also a hole scavenger. However, when C₆H₅NO₂ was added, the electrons were quenched, the reaction was still going on, although the conversion was greatly reduced. This may be because the addition of the electron scavenger effectively separated the photo-generated holes from the photo-generated electrons and reduced the recombination efficiency of electrons and holes, which played a role in promoting the reaction.